View metadata, citation and similar papers at core.ac.uk

brought to you by CORE

provided by HAL-CEA

Interface growth mechanism in Ion Beam Sputtering deposited Mo/Si multi-layers

Christophe Largeron, Etienne Quesnel, Jany Thibault

▶ **To cite this version:**

Christophe Largeron, Etienne Quesnel, Jany Thibault. Interface growth mechanism in Ion Beam Sputtering deposited Mo/Si multi-layers. Philosophical Magazine, Taylor & Francis, 2006, 86 (19), pp.2865-2880. <10.1080/14786430600640502>. <hal-00513676>

HAL Id: hal-00513676

https://hal.archives-ouvertes.fr/hal-00513676

Submitted on 1 Sep 2010

HAL is a multi-disciplinary open access archive for the deposit and dissemination of scientific research documents, whether they are published or not. The documents may come from teaching and research institutions in France or abroad, or from public or private research centers.

L'archive ouverte pluridisciplinaire **HAL**, est destinée au dépôt et à la diffusion de documents scientifiques de niveau recherche, publiés ou non, émanant des établissements d'enseignement et de recherche français ou étrangers, des laboratoires publics ou privés.

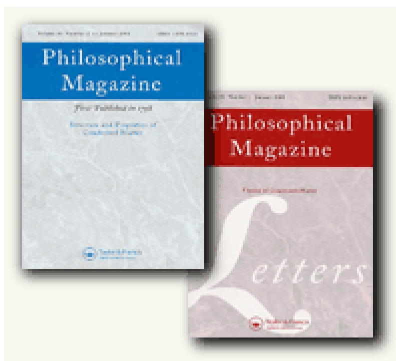

For Peer Review Only

Interface growth mechanism in Ion Beam Sputtering deposited Mo/Si multi-layers

Journal:	*Philosophical Magazine & Philosophical Magazine Letters*
Manuscript ID:	TPHM-05-Nov-0483.R2
Journal Selection:	Philosophical Magazine
Date Submitted by the Author:	06-Feb-2006
Complete List of Authors:	LARGERON, Christophe; CEA - Leti, Optronics Quesnel, Etienne; CEA, Leti, Optronics Thibault, Jany; CNRS, TECSEN
Keywords:	thin-film silicon, computer simulation, diffusion, interfacial thermodynamics, multilayer, thin-film mechanics, thin-film reactions
Keywords (user supplied):	

1
2
3
4
5
6
7
8
9
10
11
12
13
14
15
16
17
18
19
20
21
22
23
24
25
26
27
28
29
30
31
32
33
34
35
36
37
38
39
40
41
42
43
44
45
46
47
48
49
50
51
52
53
54
55
56
57
58
59
60

Interface growth mechanism in Ion Beam Sputtering deposited Mo/Si multi-layers.

Christophe Largeron*, Etienne Quesnel* and Jany Thibault**

*LETI/CEA.G-DOPT- 17 rue des Martyrs, 38054 Grenoble cedex 9, France.
C. Largeron : telephone number : 33 (0)4 38 78 42 95 – fax number : 33 (0)4 38 78 51 67 - email : clargeron@sorbier.cea.fr
E. Quesnel : telephone number : 33 (0)4 38 78 33 22 – fax number :33 (0)4 38 78 50 46 - email : quesnel@chartreuse.cea.fr

*** Laboratoire TECSEN, UMR 6122 CNRS, Case 262 - Université Aix-Marseille III, Paul Cézanne - Faculté des Sciences et Techniques de St Jérôme - 13397 Marseille, France.*
Telephone number : 33 (0)4 91 28 90 87 – email : jany.thibault@univ.u-3mrs.fr

For Peer Review Only

ABSTRACT

Despite the technological importance of Metal/Si multilayer structure in Microelectronics, the interface reactions occurring during their preparation are not fully understood, yet. In this work, the interface intermixing in Mo/Si multilayer coatings has been studied with respect to their preparation conditions. Various samples prepared at room temperature with different Mo deposition rates (0.06-0.43 Å/s) and a constant Si one have been investigated by detailed TEM observations. Contrary to the Si-on-Mo interface where no evidence of chemical intermixing could be found, the Mo-on-Si interface presents a noticeable interface zone whose thickness was found to noticeably decrease (from 4.1 to 3.2 nm) when increasing the Mo deposition rate. Such intermixing phenomena correspond to diffusion mechanisms having coefficients ranging from $0.25.10^{-15}$ to $1.2.10^{-15}$ cm²/s at room temperature. By assuming a diffusion mechanism mainly driven by Mo-Si atomic exchanges to minimize the surface energy, the diffusion dependence with Mo deposition rate has successfully simulated using a cellular automaton. A refined simulation including Mo cluster formation is also proposed to explain the scenario leading to the full crystallisation of Mo layers.

Key-words : Mo/Si, EUV, ion beam sputtering, interface, diffusion coefficient, cellular automaton.

Author to be contacted: C. Largeron (clargeron@sorbier.cea.fr)

1
2
3
4
5
6
7
8
9
10
11
12
13
14
15
16
17
18
19
20
21
22
23
24
25
26
27
28
29
30
31
32
33
34
35
36
37
38
39
40
41
42
43
44
45
46
47
48
49
50
51
52
53
54
55
56
57
58
59
60

INTRODUCTION

Mo-Si multilayer coatings are being intensively investigated as the most suitable materials for the extreme ultraviolet (EUV) reflectors which will equip the future EUV lithography tools [1]. These tools are expected to satisfy the demands of miniaturization of integrated circuits around 2010. However, some of the properties of Mo-Si multilayer stacks still need to be improved such as insufficient optical reflectance or poor thermal stability. Depending on their use in the lithography tool as light transport mirror, source light condenser or lithography mask, the multilayer coatings are currently deposited by ion assisted evaporation (IAE), magnetron (MS) or ion beam sputtering (IBS). Because of the need of defect free multilayer coatings, the IBS technique is preferentially used for the production of EUV mask blanks [2].

Much research work has been focused on EUV reflectance (R_{EUV}) improvement at the wavelength of 13.4 nm in an attempt to bring the reflectance as close as possible to the theoretical value of 74% [3]. A comparison of data published this last ten years shows that the maximum R_{EUV} value is strongly process dependent, with the highest reflectance (70%) obtained by IAE [4], intermediate values ranging from 65 to 68% by MS technique [5] and lower values comprised between 58 and 65% by IBS technology [6]. Besides, using IBS techniques, specific deposition parameters like sputtering gas were also found to greatly affect the optical properties of Mo-Si coating [6]

One of the reasons of this dependency is that each kind of process with its associated deposition condition leads to multilayer coatings having more or less gradual internal interface zones which strongly impact the final EUV reflectance. The way this interface zone forms during deposition and the conditions which promote this formation are not today clearly identified. Different mechanisms explaining the Mo-Si intermixing are proposed, like thermal diffusion [7] or Mo implantation resulting from the high energy of depositing Mo

For Peer Review Only

1
2
3
4
5
6
7
8
9
10
11
12
13
14
15
16
17
18
19
20
21
22
23
24
25
26
27
28
29
30
31
32
33
34
35
36
37
38
39
40
41
42
43
44
45
46
47
48
49
50
51
52
53
54
55
56
57
58
59
60

adatoms [8]. Nevertheless, none of these explanations can explain in a satisfying manner the results obtained, in particular, with IBS. For instance, how can we explain that changing the ion species can improve so much the reflectance? Is there any limitation inherent to the IBS process itself?

The aim of the present work is to bring a better comprehension of the mechanism which drives the Mo-on-Si interface zone growth and to identify the main underlying process parameters. The roles of temperature and/or Mo adatom energy on Mo-on-Si interface zone growth are well known [8, 9]. Their increase makes the interface zone to be thicker. In return, a deposition at room temperature and low energy (evaporation) does not prevent from having any Mo-Si interdiffusion. This result supports the idea that another process parameter could be involved in the Mo-on-Si interface zone formation.

In the present work, on the basis of growth simulation results, the deposition rate has been chosen as a new deposition parameter capable of affecting the Mo-on-Si interface zone growth. A set of experiments has been therefore conducted to analyse the early growth stages of thin Mo layers within IBS deposited Mo/Si stacks prepared at different deposition rates. The interface observations were made by high-resolution transmission electron microscopy (HRTEM) and energy filtering TEM (chemical analysis).

In the following sections, after a brief description of the experimental procedure to prepare and characterize the coatings, the computing model used for simulation will be presented. Then, experimental results will be detailed and compared to predictions in order to check the validity of model and its assumptions regarding the Mo-Si intermixing mechanism.

For Peer Review Only

1
2
3
4
5
6
7
8
9
10
11
12
13
14
15
16
17
18
19
20
21
22
23
24
25
26
27
28
29
30
31
32
33
34
35
36
37
38
39
40
41
42
43
44
45
46
47
48
49
50
51
52
53
54
55
56
57
58
59
60

EXPERIMENTAL PROCEDURE

A. Sample preparation and characterisation

To study the early growth stages of Mo layers deposited on silicon layers, specific multilayer samples were prepared. They consist in a periodic stack having silicon layers of constant thickness alternatively deposited with Mo layers of slightly increasing thickness as shown in table I. They mainly differ each other by the deposition rate of molybdenum which was varied either by reducing the ion density of sputtering beam or by changing the ion species. The t_{Mo} values indicated in Table I corresponds to the calculated thickness of Mo (deposition rate multiplied by time of deposition). The deposition rate (R) of silicon was about the same whatever the sample. It must be noted that due to a programming mistake a thicker (150 Å) Si layer has been inserted between layer 6 and 7 in sample C1 and between substrate and layer 1 in sample C2. The film deposition was performed in a load-locked IBS chamber equipped with two cryogenic pumps leading to a base pressure of 4.10^{-8} mbar. The molybdenum and silicon targets were sputtered by 1000eV- accelerated ions (Ar^+ or Xe^+) at a pressure of 5.10^{-5} mbar.

To calibrate the deposition rate, preliminary deposition runs of Si on Mo bilayers were performed and characterized by grazing X-ray reflectance measurements using a SIEMENS D500 X-ray diffractometer with CuKα radiation. By comparison with simulated curves, it enabled to determine the thickness of both, Mo and Si single layers and consequently the corresponding deposition rate with an accuracy better than $\Delta R/R = \pm 5\%$.

The microstructure of multi-layer stacks was analysed by HRTEM performed on a JEOL 4000EX microscope having a resolution ranging from 0.12 to 0.17 nm. For some samples, additional energy filtering TEM analyses were made using a JEOL 3010 microscope with an imaging resolution of 0.17 nm and a spatial resolution of 0.5 nm for the chemical profiles.

For Peer Review Only

B. Multilayer growth simulation

The model presented here is based on the cellular automaton (CA) concept introduced by von Neumann in the 40's [10]. This kind of discrete deterministic system can be used to model physical laws like corrosion pit growth [11], crystal structures growth [12] or fluid flow [13]. Recently, Wolfram [14] pointed out the possibility to enlarge the CA concept to various domains like biology, nanomaterials or sociology.

Our CA model consists in a 2D cells grid (see figure 1c) where each cell can take one of the two possible atomic states: either molybdenum or silicon atom. Before starting the simulation, the grid only comprises the substrate layer and empty cells on top of it (no deposited layer). The substrate layer is made of Si or Mo cells. To simulate material deposition, for instance Mo deposition on Si, at each time step, some of the empty cells, randomly chosen on the top of the grid first switch to Mo state, then fall onto the Si substrate layer. Afterwards, each cell of the grid updates its current state according to transition rules which take into account the four nearest neighbour cells and itself. The rules can be balanced according to the interaction weight (W) we like to give to cells neighbourhood. We consider two evolutionary states (Si and Mo) and a basic state (blank cell). There are thus 3!, namely 6 types of different interactions. A matrix of exchange 3x3, noted W(C1, C2) can be thus built, which gives the level of interaction between two close cells C1 and C2 (see Table II). The higher W(C1, C2) is, the more predominant the interaction between the two cells is.

Considering C(x,y) as a function giving the states of the cell located at the (x,y) position, the occurrence of cell exchange will depend on the value taken by the two following functions : A^{be} before exchange and A^{ae} after exchange.

$$A^{be} = \sum_{j=y-1}^{y+1} \sum_{i=x-1}^{x+1} W\left[C(x,y), C(i,j)\right] + \sum_{j=y-2}^{y} \sum_{i=x-1}^{x+1} W\left[C(x,y-1), C(i,j)\right] - W\left[C(x,y), C(x,y-1)\right]$$

$$A^{ae} = \sum_{j=y-1}^{y+1} \sum_{i=x-1}^{x+1} W\left[C(x,y-1), C(i,j)\right] + \sum_{j=y-2}^{y} \sum_{i=x-1}^{x+1} W\left[C(x,y), C(i,j)\right] - W\left[C(x,y), C(x,y-1)\right]$$

and W[C(x,y), C(x,y)] = 0

1
2
3
4
5
6
7
8
9
10
11
12
13
14
15
16
17
18
19
20
21
22
23
24
25
26
27
28
29
30
31
32
33
34
35
36
37
38
39
40
41
42
43
44
45
46
47
48
49
50
51
52
53
54
55
56
57
58
59
60

The exchange takes place when :

$$A^{ae} > A^{be}$$

In our model, the criteria of cell modification are based on two different effects:

- The surfactant effect (SE):

This is the main effect. It is possible to show that a minimization of the surface energy can induce an atomic exchange at the surface [15]. This effect could happen in the Mo-Si multilayer, which would explain the asymmetry observed between the two interfaces Mo-on-Si and Si-on-Mo. Thus, when considering Mo deposition on a Si layer, the surfactant effect leads to the exchange of one silicon cell (from the substrate layer) with the "falling" molybdenum cell at the surface (see figure 1a). However, when the falling molybdenum cell is environed with 4 cells (Mo or Si), the exchange mechanism stops.

- The chemical effect (CE):

The strong chemical affinity between silicon and molybdenum leads to the formation of a silicide compound (amorphous or crystalline). We model this chemical affinity using a numerical law which optimizes links between the Mo and Si cells. The more stable pattern is obtained when four silicon cells surround one molybdenum cell (or four molybdenum cells around one silicon cell). Without any other transition rule, this effect leads to a checkerboard-like pattern constituted by Mo and Si cells (see figure 1b).

The reference weight W=1 is allotted to the connection between a Si cell and a blank cell. The presence of a Si cell at the surface is thus promoted in order to encourage the surfactant effect SE (minimization of the energy of surface). It is observed that for W(Si, Mo) > 0.6, SE is not implemented any more and only CE drives the evolution of the automat. As a consequence, to

http://mc.manuscriptcentral.com/pm-pml

For Peer Review Only

1
2
3
4
5
6
7
8
9
10
11
12
13
14
15
16
17
18
19
20
21
22
23
24
25
26
27
28
29
30
31
32
33
34
35
36
37
38
39
40
41
42
43
44
45
46
47
48
49
50
51
52
53
54
55
56
57
58
59
60

preserve our initial assumption, the interaction between a Si and a Mo cell is fixed at the value of 0.5 (see Table II).

The cellular automaton was developed on Microsoft Excel application using the Visual Basic Application language. When depositing molybdenum on silicon, the only variable is the number of falling Mo cells at each step, namely the number of depositing Mo atoms per time step (N_{Mo}). This value can be directly compared to the experimental molybdenum deposition rate R_{Mo}. The CA simulation gives access to both output data, the thickness τ_c of the Mo-on-Si interface zone, which corresponds to the silicon diffusion length (see figure 1c) and the propagation time of the interface t_p. Moreover, as basic results, the CA simulation tool provides a graphic representation of Mo and Si interdiffusion and the corresponding Mo or Si concentration profiles along the interface zone growing direction.

To summarize, table III shows how the different parameters are involved in the experiments and in the simulation. It must be noted that N_{Mo} is strictly proportional to R_{Mo} (same constant of proportionality in the whole studied range of deposition rate).

For Peer Review Only

1 2 3 4 5 6 7 8 9 10 11 12 13 14 15 16 17 18 19 20 21 22 23 24 25 26 27 28 29 30 31 32 33 34 35 36 37 38 39 40 41 42 43 44 45 46 47 48 49 50 51 52 53 54 55 56 57 58 59 60

RESULTS

Experimental data

Before analysing in details the kinetics of Mo-on-Si interface zone formation, we first present in figure 2 a typical chemical profile of an IBS deposited Mo-Si multilayer in association with the corresponding EFTEM image. The profile which gives the silicon concentration across the 3 layer-stack Mo-Si-Mo has been scanned in the area delimited by the white rectangle of figure 2b and from the bottom to the top (opposite to the direction of coating deposition). As already reported in a previous paper [6], the EFTEM image is characteristic of sputtered Mo-Si mirrors with asymmetrical interfaces. The chemical profile exhibits two noticeable features: (i) at Si-on-Mo interface (section AB), a regular increase in Si concentration, (ii) at Mo-on-Si interface (section CDE), a plateau preceded by a steep drop in Si concentration and followed by a shallower decrease in Si concentration. This plateau suggests the formation of a chemical compound at the Mo-on-Si interface. In return, the shape of the AB profile at the Si-on-Mo interface results from the wavy Si on Mo interface alone and the integration of signal along the width of the scanned area. There is no evidence of a chemical Mo-Si intermixing at this interface.

To illustrate the progressive growth of the Mo-on-Si interface zone, figures 3a and 3b, present the HRTEM cross-section micrographs of samples C1 and C2, respectively. In these samples, the thickness of Mo layers was progressively increased until reaching the full crystallisation of Mo layers. In figure 3a, the first deposited Mo layers (close to the Si substrate) which initially should have a thickness of a few angströms look much broader, as if they were diluted in the Si matrix. A detail of such Mo layers (figure 4) shows that they consist in an amorphous Mo-Si matrix in which some nano-crystallites are embedded. The crystallites were highlighted by a numerical treatment based on a phase mapping and inversed Fourier transformation.

For Peer Review Only

1
2
3
4
5
6
7
8
9
10
11
12
13
14
15
16
17
18
19
20
21
22
23
24
25
26
27
28
29
30
31
32
33
34
35
36
37
38
39
40
41
42
43
44
45
46
47
48
49
50
51
52
53
54
55
56
57
58
59
60

The complete crystallisation of Mo layer requires to deposit between 19.2 and 21.6 Å of molybdenum (layer N° 7 and 8 in figure 3b). Layer N°7 is only partially crystallised.

According to Bajt model [16], we assume that the crystallization of the Mo deposited layer is reached when the Si concentration across the growing interface layer is lower than a limit value noted γ (limit of solubility of Si in Mo). The nucleation of Mo crystallites is thus expected to be affected by the diffusion of Si atoms, which should stop when the Mo layer entirely crystallizes. This edge point corresponds simultaneously to the deposition of a critical thickness τ_{Mo} of Mo, the formation of a critical thickness of Mo-on-Si interface zone τ_c (equivalent of the Si diffusion length) and a deposition time $t_p=\tau_{Mo}/R_{Mo}$.

To reach this point of Mo crystallization, as precisely as possible, the experimental procedure consists in successively depositing Mo layers having slightly increasing thickness, as mentioned in Table I. The measurement of the interface zone thickness on the HRTEM cross-section micrographs, before and after the amorphous to crystalline transition, gives access to the critical thickness $\tau_c=(\tau_c^{after}+\tau_c^{before})/2$, with an error range equal to the depositing thickness step. From calculation, other parameters are deduced : i) the critical thickness of deposited Mo $\tau_{Mo}=(\tau_{Mo}^{after}+\tau_{Mo}^{before})/2$, ii) the sputtering time $t_p=(t_p^{after}+t_p^{before})/2$, iii) the interface layer growth rate $R_i=\tau_c/t_p$ and iv) an estimation of the Mo-Si interdiffusion coefficient $D=\tau_c^2/(2*t_p)$. The values obtained for the different samples are listed in Table IV. We observe that the Si diffusion length τ_c increases when the deposition rate R_{Mo} decreases. At the same time, the mean growth rate of Mo-on-Si interface (R_i) is found to be always higher that the deposition R_{Mo}. We even observe a rather linear dependence of R_i with R_{Mo} as shown by figure 5 ($dRi/dRMo \approx 1,7$).

Figure 6 presents the evolution of the Mo-Si interface thickness τ_c versus t_{Mo} as measured in samples C1 and C2, namely for a low deposition rate of molybdenum. The characteristics of this curve is a steep increase of τ_c when starting the Mo deposition (low t_{Mo} values) followed

For Peer Review Only

1 2 3 4 5 6 7 8 9 10 11 12 13 14 15 16 17 18 19 20 21 22 23 24 25 26 27 28 29 30 31 32 33 34 35 36 37 38 39 40 41 42 43 44 45 46 47 48 49 50 51 52 53 54 55 56 57 58 59 60

by a saturation at τ_c~ 4 nm for t_{Mo}>1nm and a sudden drop in τ_c when Mo crystallises at t_{Mo}~2nm. The continuous curve in fig.6 corresponds to the simulation given by the CA model.

Simulation data

As already mentioned in the previous section and in figure 1, the simulation of Mo deposition on Si layer leads to the generation of a 4 layer stack. In the direction of the multilayer growth, the stack successively comprises the silicon layer, a homogeneous Mo-Si layer (zone I), a second Mo-Si layer showing a decrease in Si concentration (zone II) and a pure Mo layer. Zone I, with its checkerboard-like pattern, results from the chemical effect which is predominant along a few atomic layers, only. Beyond (zone II), the distribution of Si atoms is dominated by the surfactant effect where the Si cells migrate toward the surface as the Mo cells progressively deposit. The diffusion length of Si in Mo (τ_c) corresponds then to the thickness of zone I and II.

A first qualitative result obtained by simulation is presented in figure 7. We clearly observe that the simulation predicts the shrinkage of the Si inter-diffusion layer (zone I and II) with the increase of Mo deposition rate (N_{Mo}). The thickness of zone II is particularly affected by N_{Mo} while zone I remains unchanged. In other words, the chemical effect is not affected by N_{Mo} while the surfactant effect is. That means that if we would be able to indefinitely increase N_{Mo}, the Si diffusion length τ_c should tend to a lower limit corresponding to the diffusion length related to the chemical effect only. The same trend has been observed when plotting the time of diffusion t_p versus N_{Mo} (figure 8). We indeed observe a curve showing an asymptotic behavior at both limits N_{Mo}=0 and $+\infty$. This behaviour predicted by the CA simulation is found to be in good agreement with experimental data of table III and reported in figure 8. It must be noted that the simulated curve has been fitted by a same constant factor over the whole range of Mo deposition rate. Finally, from figure 7a (lower Mo deposition rate), the simulated chemical profile of Mo-on-Si interface has been deduced (figure 9). The

http://mc.manuscriptcentral.com/pm-pml
For Peer Review Only

1 2 3 4 5 6 7 8 9 10 11 12 13 14 15 16 17 18 19 20 21 22 23 24 25 26 27 28 29 30 31 32 33 34 35 36 37 38 39 40 41 42 43 44 45 46 47 48 49 50 51 52 53 54 55 56 57 58 59 60

plateau in Si concentration which was experimentally found (figure 2) is well predicted by the CA simulation.

DISCUSSION

The main conclusion drawn from the previous results is that our CA simulation, despite its simplicity, confirms the trends observed experimentally, in particular the shape of chemical profile of the Mo-on-Si interface zone and the dependence of diffusion mechanism with the Mo deposition rate. The simulation was exclusively applied to the Mo-on-Si interface since no evidence of chemical intermixing was found in the case of Si-on-Mo interfaces.

The CA simulation implemented for this work simply assumes that the mechanism of diffusion is mainly driven by the surface energies of Si and Mo (827 and 1915 mJ/m^2, respectively) which induce a Mo-Si atomic exchange at the interface. This assumption is supported by the fact that the Mo-Si interdiffusion occurs during IBS deposition, which means at low temperature (T<60°C) where the thermal activation is negligible. Qualitatively, the simulation shows that the diffusion should be enhanced at low Mo deposition rate, which is indeed observed experimentally (figure 7). Quantitatively (figure 8), a discrepancy appears at low Mo deposition rate where the increase of time of diffusion (tp) is clearly overestimated by the model. We must keep in mind that the kinetic of diffusion provided by our CA simulation only results from Si atom displacements along the direction normal to the surface, according to rather simplified transition rules, these displacement being triggered by Mo atoms arriving at a given rate. In other words, a refinement of the transition rules based on some thermodynamic considerations would be probably necessary to better predict the kinetic of diffusion. Another reason for the quantitative mismatch is likely due to the fact that the surface diffusion and the formation of molybdenum clusters were not taken into account. At low Mo deposition rate, these mechanisms should not be neglected since the Mo atoms have

For Peer Review Only

1
2
3
4
5
6
7
8
9
10
11
12
13
14
15
16
17
18
19
20
21
22
23
24
25
26
27
28
29
30
31
32
33
34
35
36
37
38
39
40
41
42
43
44
45
46
47
48
49
50
51
52
53
54
55
56
57
58
59
60

probably enough time to laterally diffuse and segregate before Mo-Si atomic exchange occurrence.

Nevertheless, whatever the accuracy of the model, it clearly evidences that there is a competition between the deposition of Mo atoms (to form a Mo layer) and the growth of the Mo-Si interface zone. It was indeed found that the growth rate of interface zone is roughly twice the deposition rate of Mo (dRi/dRMo ≈ 1,7) and that the thickness of interface zone is related to the Mo deposition rate (τ_c decreases when R_{Mo} increases). If we consider that the interface zone has, in average, the composition of $MoSi_2$ [16], the ratio of ~1.7 is consistent with the density ratio of materials (dMo/d $MoSi_2$ =10.22/6.24 = 1.64). This result indicates that during the growth of interface zone, most Mo atoms are diluted in the interface zone to form an amorphous Mo-Si compound. Nevertheless, our TEM observations show that very small crystallized Mo grains can also form within the amorphous interface zone (figure 4). These nano-clusters of Mo act as precursors of the full crystallisation of Mo layer which stops the interface zone growth. As shown by figure 6, this Mo layer crystallisation is even associated with a sudden contraction of interface zone (thickness drop observed at τ_{Mo} ~ 2.1 nm).

All these observations are consistent with the model of interface formation proposed by Bajt et al. [16] and have been taken into account in a refined version of our CA simulation by simply adding a new concept of critical radius r* related to the crystallisation of Mo clusters. The formation of these clusters is indeed expected to occur when a minimum of Mo atoms are gathered reaching the so-called critical radius r* mentioned when dealing, for instance, with the mechanism of material nucleation in liquid phase. If we introduce in our cellular automaton this concept of critical radius r*, we are able to simulate a possible scenario for Mo layer growth when deposited on a silicon layer. In figure 10, the refined simulation result is presented for three different increasing simulation times corresponding to the three main steps of Mo layer growth:

For Peer Review Only
http://mc.manuscriptcentral.com/pm-pml

1
2
3
4
5
6
7
8
9
10
11
12
13
14
15
16
17
18
19
20
21
22
23
24
25
26
27
28
29
30
31
32
33
34
35
36
37
38
39
40
41
42
43
44
45
46
47
48
49
50
51
52
53
54
55
56
57
58
59
60

1. The first Mo atoms arrive on the pure silicon surface and form a rather homogeneous Mo-Si amorphous layer (zone I type layer). Some Si atoms can segregate at the surface.
2. With the deposition of further Mo atoms, Si atoms continue to migrate up, towards the Mo layer (surfactant effect). The probability of having zones without any silicon atoms significantly increases making possible for Mo atoms to reach the r* critical value. In this example of simulation, r* was arbitrary chosen and corresponds to six Mo atoms. Crystallised Mo clusters are forming. They are part of the thick interface zone having the apparent thickness τ_c.
3. Some Si atoms continue to migrate up and the full crystallization can occur starting from the pre-existing Mo cluster precursors.

For Peer Review Only

1 2 3 4 5 6 7 8 9 10 11 12 13 14 15 16 17 18 19 20 21 22 23 24 25 26 27 28 29 30 31 32 33 34 35 36 37 38 39 40 41 42 43 44 45 46 47 48 49 50 51 52 53 54 55 56 57 58 59 60

CONCLUSION

The evolution of Mo-Si intermixing in IBS deposited multilayer coatings has been experimentally studied for various Mo deposition rates by a step by step TEM analysis of the Mo-on-Si interface zone growth. Contrary to the Si-on-Mo interface where no evidence of chemical intermixing could be found, the Mo-on-Si interface is the seat of a noticeable interdiffusion flux even observed when the materials are deposited at room temperature. For Mo deposition rates varying from 0.06 to 0.43 Å/s, the interdiffusion coefficients were found to range from $0.25.10^{-15}$ to $1.2.10^{-15}$ cm²/s, which is relatively high. A strong dependence of the Mo-Si interdiffusion amplitude with the Mo deposition rate has been thus evidenced.

To assess the origin of such diffusion behaviour, a cellular automaton simulation has been implemented. By assuming a Mo-Si intermixing mainly driven by a mechanism of Mo-Si atomic exchanges to minimize the surface energy, the main trends of experimental results have been successfully simulated. By proposing some refinements of the model including the formation of Mo nano-crystallites embedded inside the Mo-on-Si interface zone, it has been also possible to confirm by simulation the more likely scenario leading to the full crystallisation of Mo layers.

ACKNOWLEDGMENTS:

We would like to thank Dr Fiqiri Hodaj for his fruitful contribution. We would like to thank V. Muffato for her valuable technical support regarding the coating deposition and D. Muyard for the grazing X-ray characterisations. This work was performed under the auspices of the MEFI (French Ministry of Economy, Finance and Industry) and, partially, in the framework of the EXTUMASK MEDEA+ project.

For Peer Review Only

1
2
3
4
5
6
7
8
9
10
11
12
13
14
15
16
17
18
19
20
21
22
23
24
25
26
27
28
29
30
31
32
33
34
35
36
37
38
39
40
41
42
43
44
45
46
47
48
49
50
51
52
53
54
55
56
57
58
59
60

REFERENCES

[1] J.E. Bjorkholm ; « EUV lithography – the successor to optical lithography ?», *Intel Technology Journal*, **Vol. Q3 1998**

[2] J. Hue, E. Quesnel, V. Muffato, C. Pellé, D. Granier, S. Favier and P. Besson, *Microelect. Eng*, **61-62**, 2002, pp 203-211

[3] S. Braun, H. Mai, M. Moss, R. Scholz and A. Leson ; « Mo/Si Multilayers with Different Barrier Layers for Applications as Extrem Ultraviolet Mirrors », *Jpn. Journal of Applied Physics*, **Vol. 41, Part 1, No 6B**, 2002, pp 4074-4081

4 J.M. Liang, L.J. Chen ; « Interfacial reactions and thermal stability of ultrahigh vacuum deposited multiplayer Mo/Si structures », *Journal of Applied Physics*, **Vol. 79, No 8**, 1996, pp. 4072-4077

[5] P. Reining, F. Fenske, W. Fushs, A. Schöpke, B. Selle ; « Crystalline silicon films sputtered on molybdenum – a study of the silicon-molybdenum interface », *Applied surface Science*, **Vol. 210**, 2003, pp. 301-306

[6] E. Quesnel, C. Teyssier, V. Muffato, J. Thibault ; « Study of ion-beam-sputtered Mo/Si mirrors for EUV lithography mask: influence of sputtering gas », *Proceedings of the SPIE The International Society for Optical Engineering*, **Vol. 5250**, **No. 1**, février. 2004, pp. 88-98

[7] K. Holloway, K. Ba Do, R. Sinclair ; « Interfacial reactions on annealing molybdenum-silicon multilayers », *Journal of Applied Physics*, **Vol. 65**, **No**. **2**, 1989, pp. 471-480

[8] W. L. Morgan, D.B. Boercker ; « Simulating growth of Mo/Si multilayers », *Applied Physics Letter*, **Vol. 59**, **No 10**, septembre 1991, pp. 1176-1178

[9] D.G. Stearns, M.B. Stearns, Y. Cheng, J.H. Stith, N.M. Ceglio ; « Thermally induced structural modification of Mo-Si multilayers », *Journal of Applied Physics*, **Vol. 67**, **No. 5**, mars 1990, pp. 2415-2427

[10] John von Neumann, « Theory of self-reproducing Automata », University Of Illinois, Urbana, 1966

[11] B. Malki, B. Baroux ; « Computer simulation of the corrosion pit growth », *Corrosion Science*, **Vol. 47**, 2005, pp. 171-182

[12] S.V. Krivovichev, « Crystal structures ans cellular automata », *Acta Crystallographica Section A*, **Vol. A60**, 2004 , pp 257-262

[13] G.M. Crisci, R. Rongo, S. Di Gregorio, W. Spataro ; « The simulation model SCIARA : the 1991 and 201 lava flows at Mount Etna », *Journal of volcanology and geothermal research*, **Vol. 132**, 2004, pp 253-267

http://mc.manuscriptcentral.com/pm-pml
For Peer Review Only

1
2
3
4
5
6
7
8
9
10
11
12
13
14
15
16
17
18
19
20
21
22
23
24
25
26
27
28
29
30
31
32
33
34
35
36
37
38
39
40
41
42
43
44
45
46
47
48
49
50
51
52
53
54
55
56
57
58
59
60

[14] Stephen Wolfram, « A New Kind of Science », 2002

[15] T. Deutsch, P. Bayle, B. Gilles, F. Lançon, J. Thibault ; « Quantitative analysis of the deformation and chemical profiles of strained multiplayer », *Ultramicroscopy*, **Vol. 56, Issues 1-3**, 1994, pp. 94-107

[16] S. Bajt, D.G. Stearns, P.A. Kearney ; « Investigation of the amorphous-to-crystalline transition in Mo/Si multilayers », *Journal of Applied Physics*, **Vol. 90**, **No. 2**, juillet 2001, pp. 1017-1025

For Peer Review Only

1
2
3
4
5
6
7
8
9
10
11
12
13
14
15
16
17
18
19
20
21
22
23
24
25
26
27
28
29
30
31
32
33
34
35
36
37
38
39
40
41
42
43
44
45
46
47
48
49
50
51
52
53
54
55
56
57
58
59
60

Sample	Ion species	R_{Mo} (Å/s)	R_{Si} (Å/s)	Layer/stack	t_{Si} (Å)	t_{Mo} (Å)
A	Xe	0.431	0.951	10 (Mo/Si)	40.9	5, 10, 15, 20, 25, 30, 35, 40, 50, 80
B	Ar	0.333	0.797	10 (Mo/Si)	41.4	5, 10, 15, 20, 25, 30, 35, 40, 50, 80
C1	Ar	0.06	0.805	10 (Mo/Si)	80	1.2, 1.8, 2.4, 3, 3.6, 4.8, 6, 7.2, 8.4, , 9.6
C2	Ar	0.06	0.805	14 (Mo/Si)	80	9.6, 10.8, 12, 14.4, 16.8, 19.2, 21.6, 24, 26.4, 28.8, 31.2, 33.6, , 36

Table I: Process and multilayer characteristics related to TEM samples
(except between layer 6 and 7 : 150 Å in samples C1 and kC2)

For Peer Review Only

1
2
3
4
5
6
7
8
9
10
11
12
13
14
15
16
17
18
19
20
21
22
23
24
25
26
27
28
29
30
31
32
33
34
35
36
37
38
39
40
41
42
43
44
45
46
47
48
49
50
51
52
53
54
55
56
57
58
59
60

		C_1		
		Si	Mo	blank cell
C_2	Si	0	0.5	1
	Mo	0.5	0	0
	blank cell	1	0	0

Table II: Interaction weight matrix W(C1, C2) between the different cells

For Peer Review Only

1
2
3
4
5
6
7
8
9
10
11
12
13
14
15
16
17
18
19
20
21
22
23
24
25
26
27
28
29
30
31
32
33
34
35
36
37
38
39
40
41
42
43
44
45
46
47
48
49
50
51
52
53
54
55
56
57
58
59
60

Parameter	Process	TEM observation	Calculation from experiments	Cellular Automaton model
Interface thickness (Å)		τ_c		τ_c
Molybdenum deposition rate (Å/s)	R_{Mo}			$N_{Mo} \propto R_{Mo}$
Time of propagation (s)			$t_p = \tau_{Mo}/ R_{Mo}$	t_p

Table III: correspondence between experimental and simulation data.

For Peer Review Only

1 2 3 4 5 6 7 8 9 10 11 12 13 14 15 16 17 18 19 20 21 22 23 24 25 26 27 28 29 30 31 32 33 34 35 36 37 38 39 40 41 42 43 44 45 46 47 48 49 50 51 52 53 54 55 56 57 58 59 60

Sample	R_{Mo} (Å/s)	τ_c (nm)	τ_{Mo} (nm)	t_p (s)	R_i (Å/s)	D (cm²/s)
A	0,431	3,2	1,75	41	0,77	$1{,}20.10^{-15}$
B	0,333	3,7	2,25	68	0,54	10^{-15}
C2	0,06	4,1	2,03	338	0,12	$2{,}50.10^{-16}$

Table IV : Measured parameters
(HRTEM imaging resolution close to 0.2 µm)

For Peer Review Only

1
2
3
4
5
6
7
8
9
10
11
12
13
14
15
16
17
18
19
20
21
22
23
24
25
26
27
28
29
30
31
32
33
34
35
36
37
38
39
40
41
42
43
44
45
46
47
48
49
50
51
52
53
54
55
56
57
58
59
60

FIGURE CAPTIONS

Figure 1: simulation patterns showing a) the surfactant effect, b) the chemical effect and c) an example of simulation result (■ Si, ■ Mo).

Figure 2: typical chemical profile of an IBS deposited Mo-Si multilayer, and the corresponding EFTEM image.

Figure 3: TEM cross-sections of samples a) C1 and b) C2. Dark and bright layers correspond to Mo and Si layers, respectively. Sample C1 is mainly amorphous. In sample C2, the Mo layer crystallises for t_{Mo}= 21.6 Å (dark layer n° 8 pointed by a small arrow).

Figure 4: detailed TEM characterisation of Mo-Si layer. Isolated nano-crystals of Mo have been evidenced in layer 6 of sample C1.

Figure 5: interlayer growth rate R_i versus Mo deposition rate R_{Mo}.

Figure 6: Mo-Si interface thickness versus t_{Mo} as measured in samples C1 and C2.

Figure 7: qualitative result obtained by AC simulation. From left to right, the N_{Mo} value has been increased by an order.

Figure 8: propagation time of the interface t_p versus the Mo deposition rate. Semi-quantitative results obtained by AC simulation and experimental data.

Figure 9: simulated chemical profile of Mo-on-Si interface, corresponding to fig. 7a.

Figure 10 : refined simulation of Mo on Si deposition taking into account the Mo grains crystallisation.

For Peer Review Only

1
2
3
4
5
6
7
8
9
10
11
12
13
14
15
16

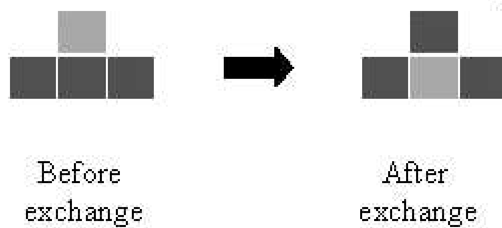

66x32mm (96 x 96 DPI)

17
18
19
20
21
22
23
24
25
26
27
28
29
30
31
32
33
34
35
36
37
38
39
40
41
42
43
44
45
46
47
48
49
50
51
52
53
54
55
56
57
58
59
60

For Peer Review Only

1
2
3
4
5
6
7
8
9
10
11
12
13
14
15
16
17
18
19
20
21
22
23
24
25
26
27
28
29
30
31
32
33
34
35
36
37
38
39
40
41
42
43
44
45
46
47
48
49
50
51
52
53
54
55
56
57
58
59
60

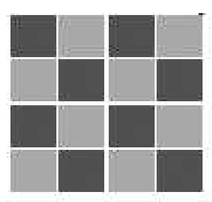

Optimized pattern

34x35mm (96 x 96 DPI)

Peer Review Only

1
2
3
4
5
6
7
8
9
10
11
12
13
14
15
16
17
18
19
20
21
22
23
24
25
26
27
28
29
30
31
32
33
34
35
36
37
38
39
40
41
42
43
44
45
46
47
48
49
50
51
52
53
54
55
56
57
58
59
60

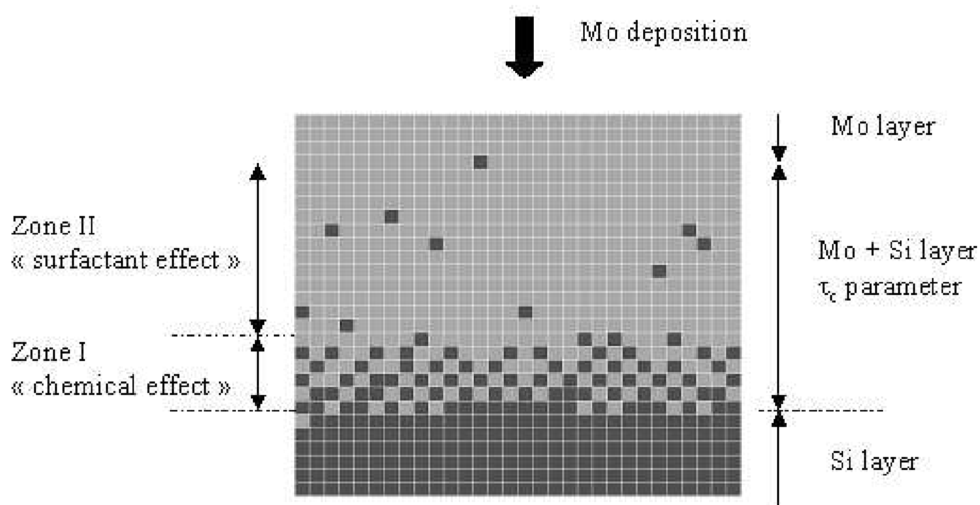

140x71mm (96 x 96 DPI)

Review Only

1
2
3
4
5
6
7
8
9
10
11
12
13
14
15
16
17
18
19
20
21
22
23
24
25
26
27
28
29
30
31
32
33
34
35
36
37
38
39
40
41
42
43
44
45
46
47
48
49
50
51
52
53
54
55
56
57
58
59
60

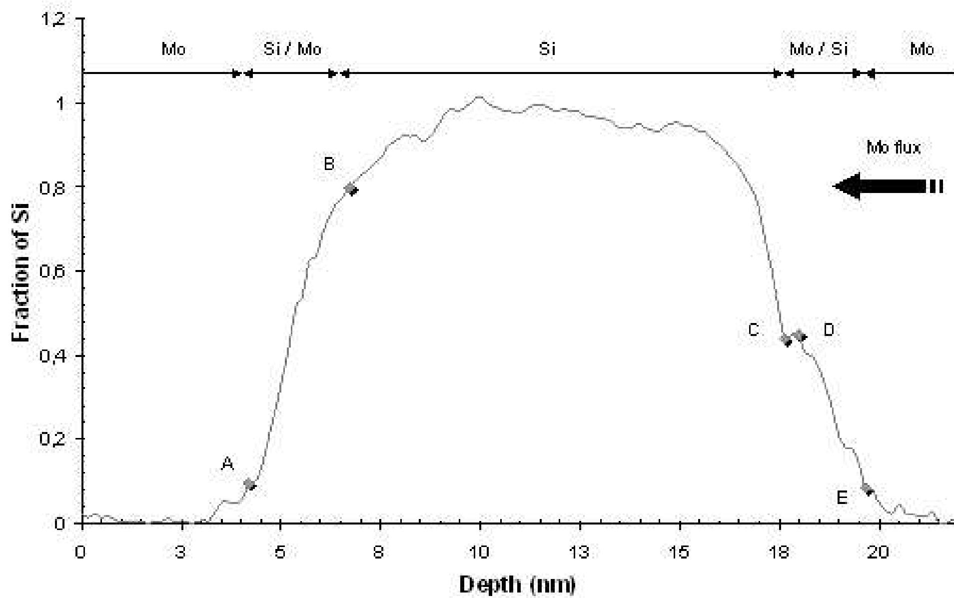

140x87mm (96 x 96 DPI)

eview Only

1
2
3
4
5
6
7
8
9
10
11
12
13
14
15
16
17
18
19
20
21
22
23
24
25
26
27
28
29
30
31
32
33
34
35
36
37
38
39
40
41
42
43
44
45
46
47
48
49
50
51
52
53
54
55
56
57
58
59
60

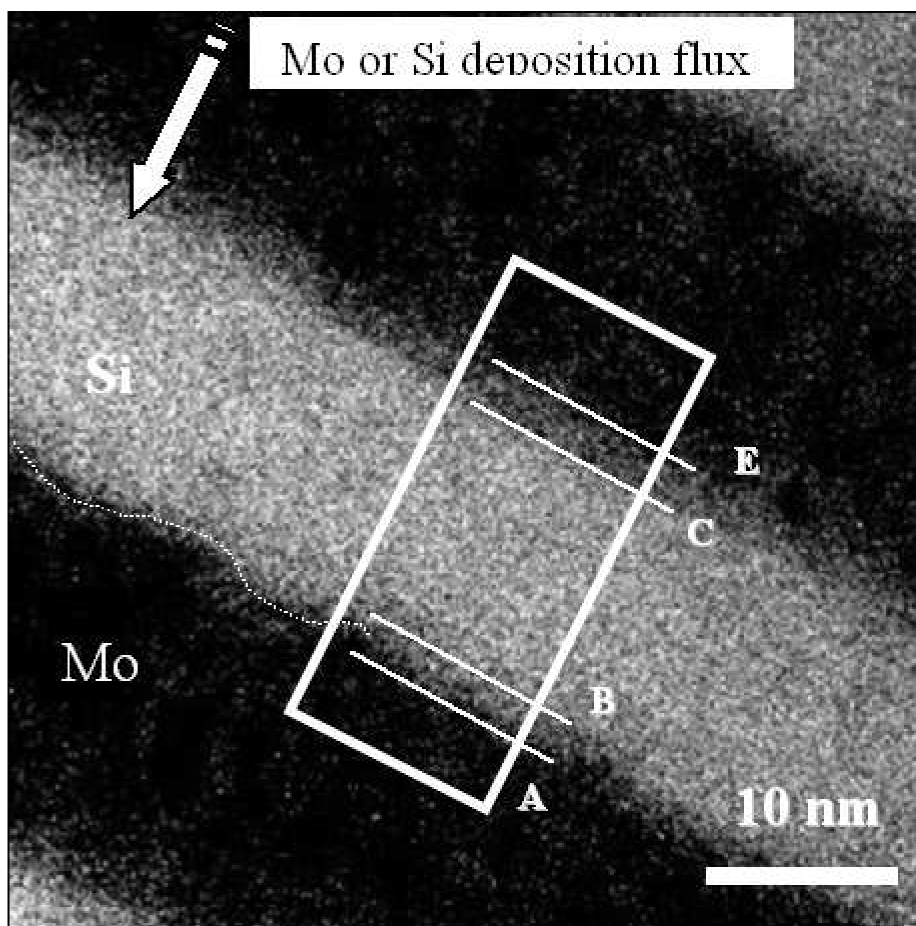

Only

1
2
3
4
5
6
7
8
9
10
11
12
13
14
15
16
17
18
19
20
21
22
23
24
25
26
27
28
29
30
31
32
33
34
35
36
37
38
39
40
41
42
43
44
45
46
47
48
49
50
51
52
53
54
55
56
57
58
59
60

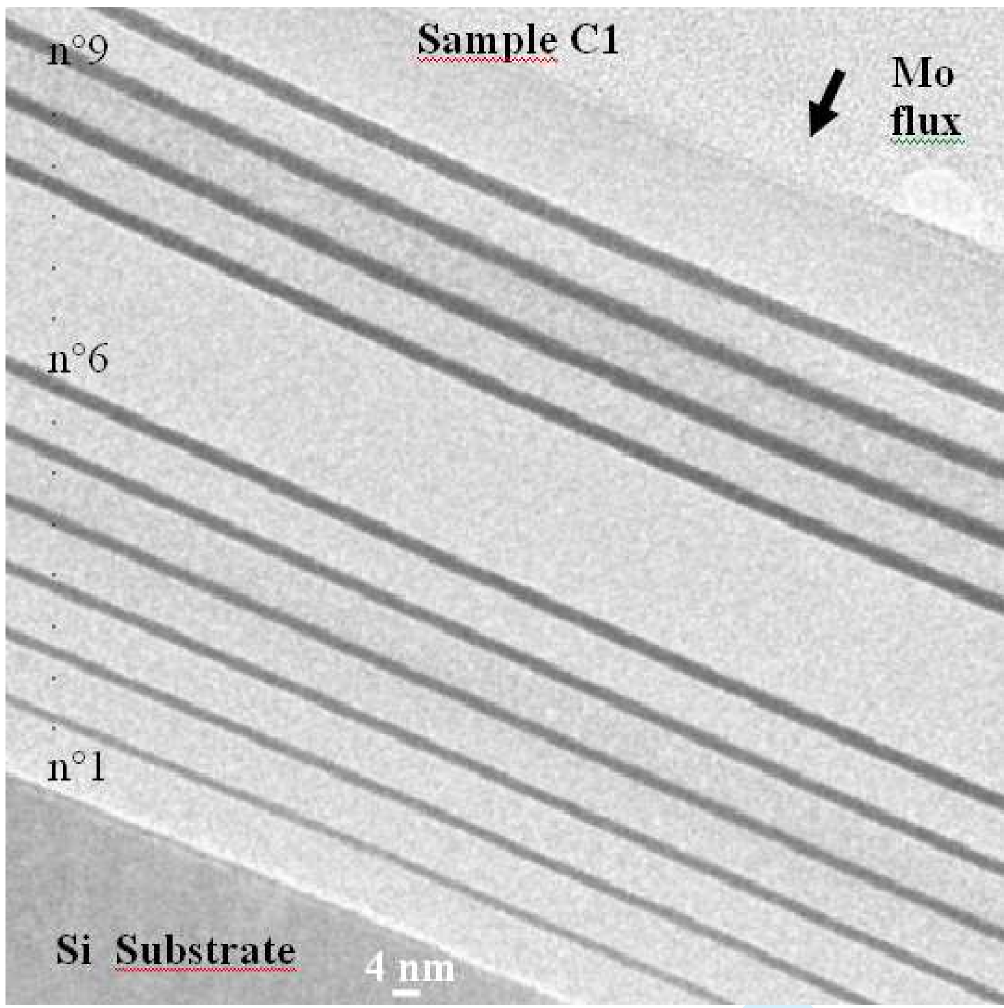

Only

1
2
3
4
5
6
7
8
9
10
11
12
13
14
15
16
17
18
19
20
21
22
23
24
25
26
27
28
29
30
31
32
33
34
35
36
37
38
39
40
41
42
43
44
45
46
47
48
49
50
51
52
53
54
55
56
57
58
59
60

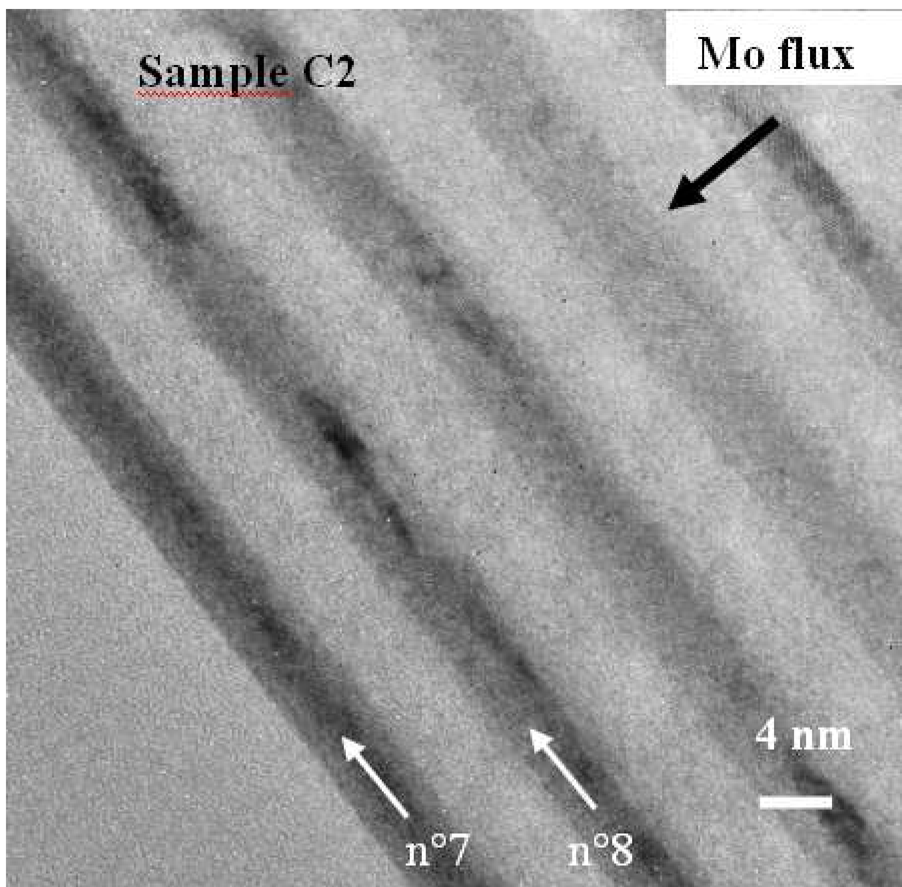

ew Only

1 2 3 4 5 6 7 8 9 10 11 12 13 14 15 16 17 18 19 20 21 22 23 24 25 26 27 28 29 30 31 32 33 34 35 36 37 38 39 40 41 42 43 44 45 46 47 48 49 50 51 52 53 54 55 56 57 58 59 60

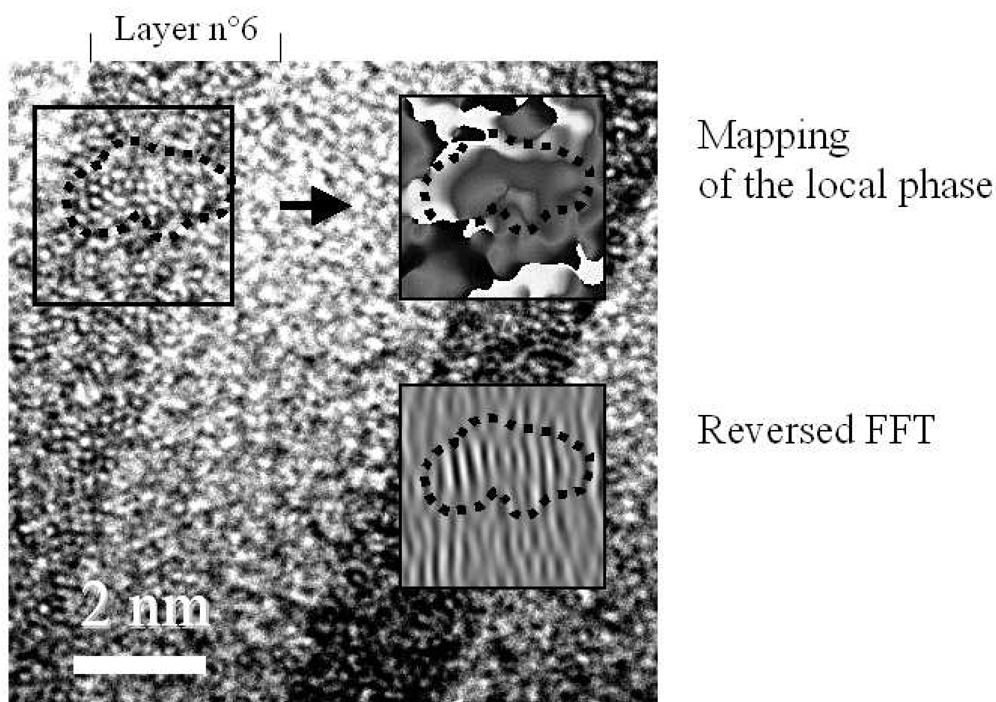

For Peer Review Only

1
2
3
4
5
6
7
8
9
10
11
12
13
14
15
16
17
18
19
20
21
22
23
24
25
26
27
28
29
30
31
32
33
34
35
36
37
38
39
40
41
42
43
44
45
46
47
48
49
50
51
52
53
54
55
56
57
58
59
60

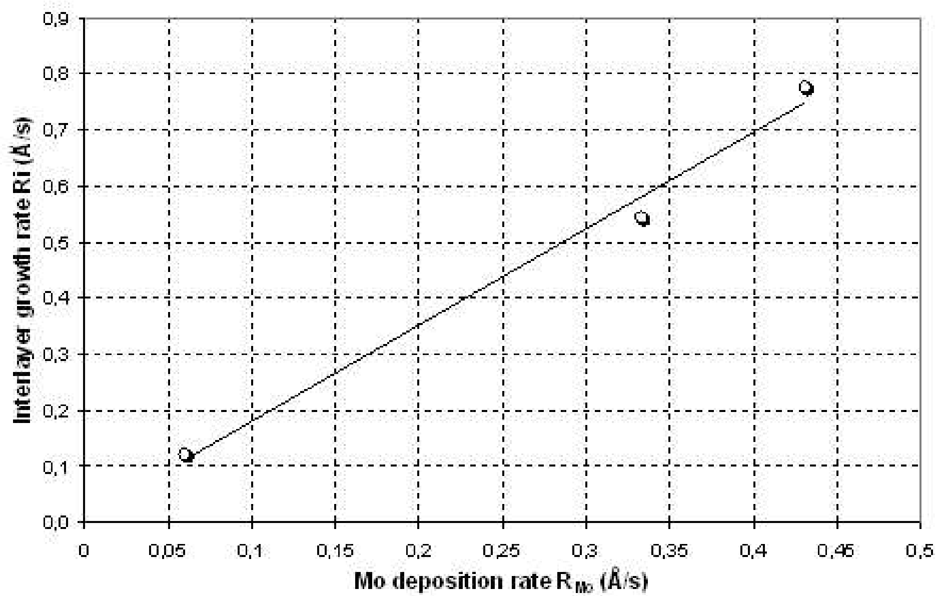

140x87mm (96 x 96 DPI)

eview Only

1
2
3
4
5
6
7
8
9
10
11
12
13
14
15
16
17
18
19
20
21
22
23
24
25
26
27
28
29
30
31
32
33
34
35
36
37
38
39
40
41
42
43
44
45
46
47
48
49
50
51
52
53
54
55
56
57
58
59
60

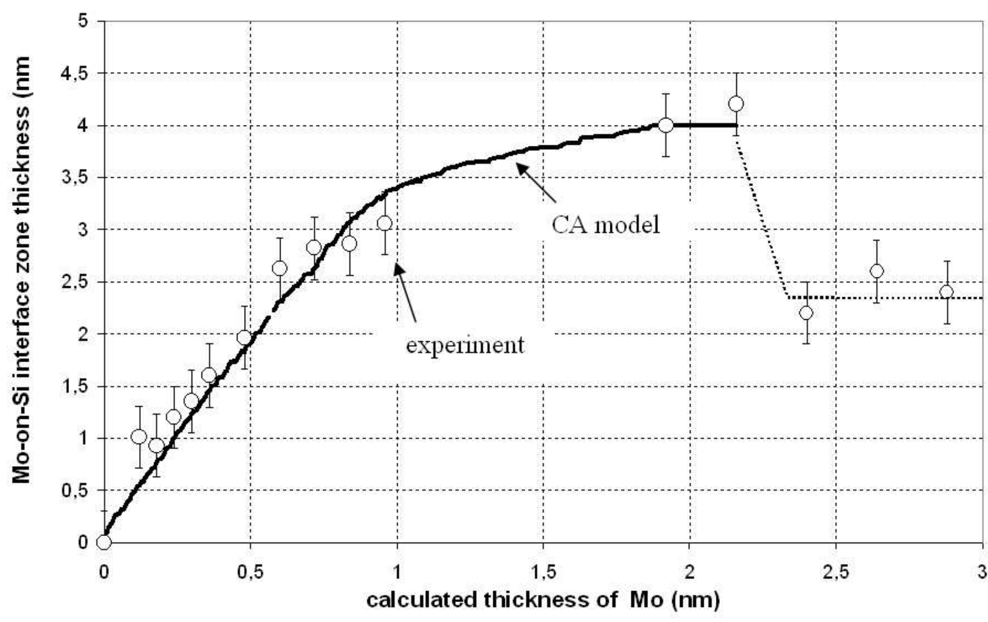

Review Only

1
2
3
4
5
6
7
8
9
10
11
12
13
14
15
16
17
18
19
20
21
22
23
24
25
26
27
28
29
30
31
32
33
34
35
36
37
38
39
40
41
42
43
44
45
46
47
48
49
50
51
52
53
54
55
56
57
58
59
60

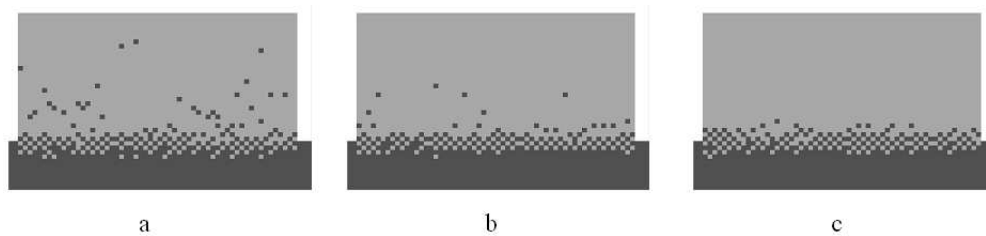

For Peer Review Only

1
2
3
4
5
6
7
8
9
10
11
12
13
14
15
16
17
18
19
20
21
22
23
24
25
26
27
28
29
30
31
32
33
34
35
36
37
38
39
40
41
42
43
44
45
46
47
48
49
50
51
52
53
54
55
56
57
58
59
60

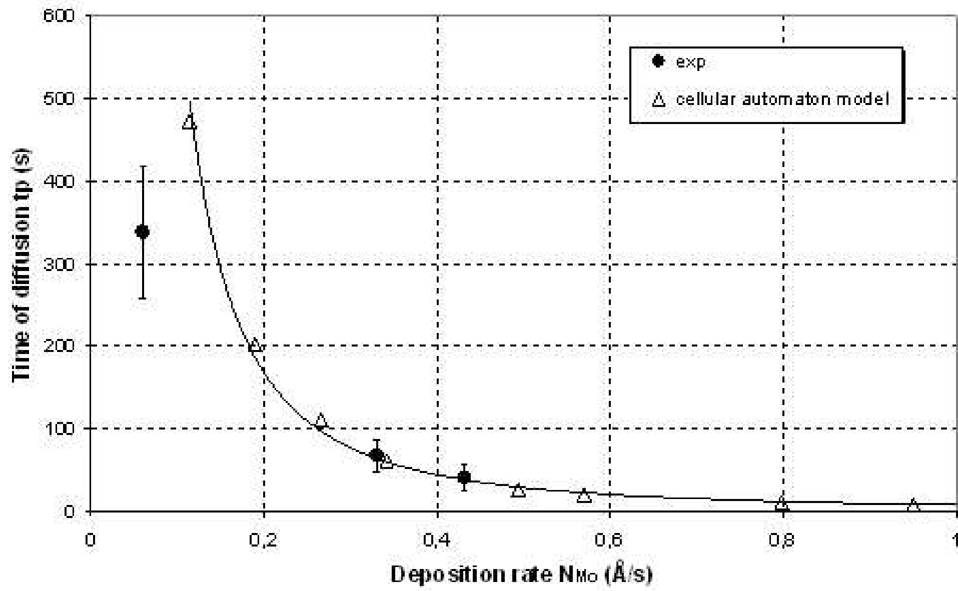

140x87mm (96 x 96 DPI)

review Only

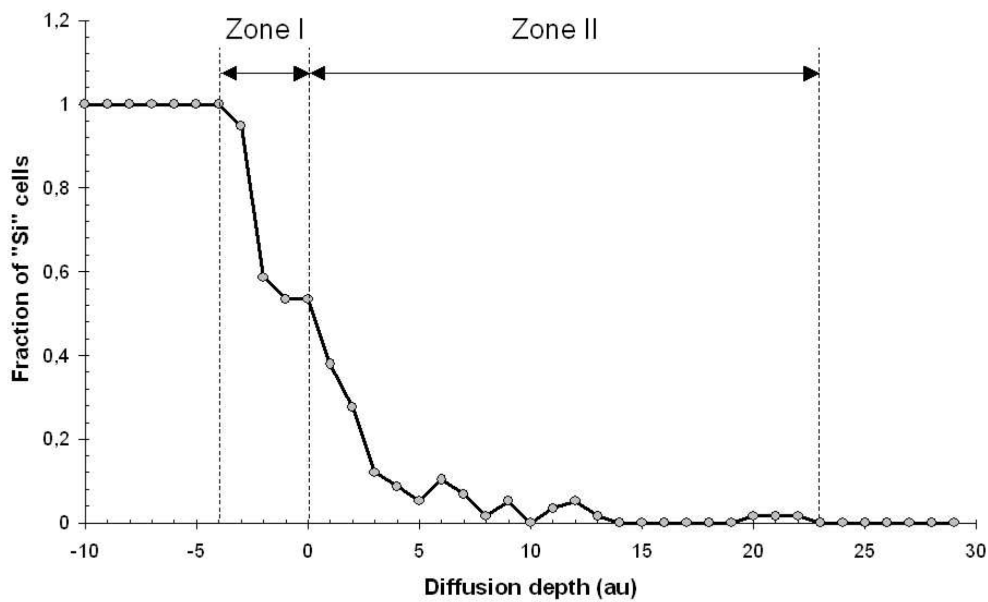

Review Only

1
2
3
4
5
6
7
8
9
10
11
12
13
14
15
16
17
18
19
20
21
22
23
24
25
26
27
28
29
30
31
32
33
34
35
36
37
38
39
40
41
42
43
44
45
46
47
48
49
50
51
52
53
54
55
56
57
58
59
60

a)

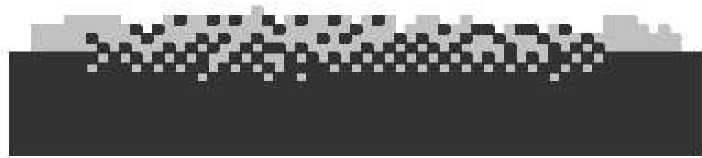

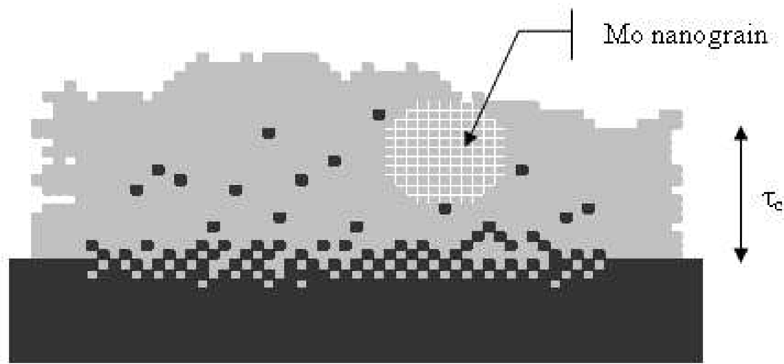

b)

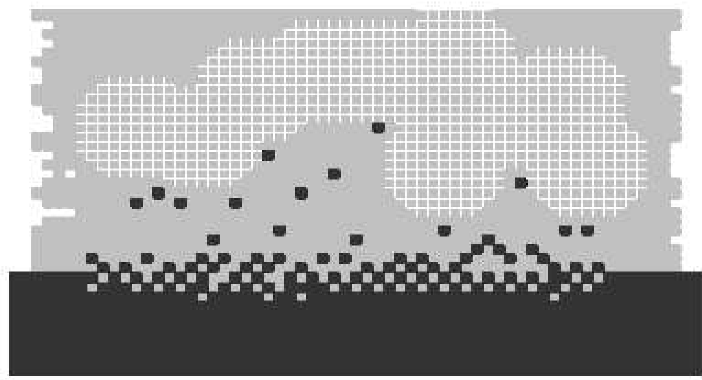

c)